Front. Optoelectron. 2017, 10(4): 395–401
DOI 10.1007/s12200-017-0735-3

RESEARCH ARTICLE

Synthesis of porous TiO_2 nanowires and their photocatalytic properties

Yonglun TANG[1], Haibo REN[2], Jiarui HUANG (✉)[2]

1 Department of Fundamental Course Teaching, Anhui Technical College of Industry and Economy, Hefei 230051, China
2 College of Chemistry and Materials Science, Anhui Normal University, Wuhu 241000, China

Abstract Porous titanium dioxide (TiO_2) nanowires were synthesized via a surfactant-free hydrothermal method followed by acid-washing process and calcination. The structures and morphologies of products were characterized by field emission scanning electron microscopy (FESEM), Transmission electron microscopy (TEM), X-ray diffraction (XRD), and Brunauer-Emmett-Teller (BET) N_2 adsorption-desorption analyses. The analysis of FESEM suggested the precursor was composed of a vast of uniform nanostructures like wires. The nanowire-like precursor was transformed into the porous nanowire after acid-treatment and calcination at 500°C for 2 h in air. The surface area of as-synthesized TiO_2 nanowires calculated by BET is 86.4 m^2/g. Furthermore, the photocatalytic properties of synthesized porous TiO_2 nanowires were evaluated through the degradation of methylene blue (MB) and Rhodamine B (RhB). The results clearly suggested that the as-prepared porous TiO_2 nanowires showed remarkable photocatalytic performance on the degradation of RhB and MB due to their small size of nanocrystallites and the porous naonstructure.

Keywords titanium dioxide (TiO_2), nanowire, porous, photocatalyst, photocatalytic performance

1 Introduction

These days, water pollution has been a major global issue and become more and more serious as the industry develops rapidly. A great number of efforts have been made to develop several approaches including biodegradation, oxidative decomposition and photochemical degradation, for the purpose of removing the organic pollutants [1]. As for the degradation of organic pollutants, semiconductor photocatalysts have been acting as a vital role. As is known to us, titanium dioxide (TiO_2), which belongs to the typical semiconductor of *n*-type, has been widely investigated due to its unique properties of high durability, high chemical stability and long-term thermal stability, which possess an extensive range of promising applications in photocatalysis [2–4], environmental pollution control [5], and solar energy conversion [6]. Concerning to the practical application of TiO_2 served as photocatalyst, it is well known that the photocatalytic activity of titanium dioxide largely depends on its crystalline structure, surface area, grain size, and defects, etc. Due to the most reactions usually taking place on the surface of TiO_2, the properties are strongly related to the local microstructures and specific surface area [7,8].

In recent years, remarkable efforts have dedicated to the preparation of various nanostructured TiO_2, including nanowires [9], nanorods [10], nanobelts [11], nanotubes [12], ultra-thin nanosheets [13], porous nanospheres [14], and nanoflowers [15], etc. Among these kinds of nanostructures, one-dimensional (1D) structure has been recognized to be the most suitable catalyst and blocks for the construction of nanoscale photocatalyst due to its unique 1D morphology with high specific surface area and the excellent physical and chemical properties conducive to promote the transport and separation of electron. For example, Lai et al. reported single crystalline TiO_2 nanowires with enhanced photocatalytic degradation of dyes [16]. Yao et al. prepared Ag-doped TiO_2 nanowires with excellent photocatalytic by sunlight induced reduction [17]. Bakar et al. synthesized N-doped TiO_2 nanorods using hydrothermal treatment with high photocatalytic activity [18]. It's well known to us that the structures with small size nanocrystallites and large specific surface area not only inhibit the recombination rate of holes and photoelectrons, but provide much more active reaction sites, which greatly enhance the efficiency of light-

Received May 15, 2017; accepted August 8, 2017

E-mail: jrhuang@mail.ahnu.edu.cn

harvesting, showing the excellent photocatalytic activity. Therefore, despite the great efforts contributed by many groups, seeking strategies for constructing the architecture of TiO_2 1D nanostructures with high surface area and specific morphology has still been an attractive ongoing task.

In present work, porous TiO_2 nanowires composed of nanocrystallites were successfully achieved by a hydrothermal method followed by acid-washing and calcination process. The photocatalytic performance of the as-prepared porous TiO_2 nanowires was also studied. The products exhibit much remarkable performance on photocatalytic decomposition of Rhodamine B (RhB) and methylene blue (MB), which is ascribed to their small size of nanocrystallites and the porous naonstructure.

2 Experimental

2.1 Synthesis

All chemicals in this experiment belonged to analytical grade and need not to be further purified. The detailed synthesis process of the porous TiO_2 nanowires like this: 0.3 g ammonium hexafluorotitanate [$(NH_4)_2TiF_6$] was dissolved in 40 mL aqueous solution of sodium hydroxide (NaOH, 1.0 M[1)]). The mixture solution was put into a Teflon-lined autoclave (50 mL) and then kept at 240°C for 5 h. The obtained white precipitate was washed with deionized water for 5 times. After that, the white precipitate was immersed in 0.1 M HCl solution and placed at 28°C for 24 h. Subsequently, the products were washed with deionized water for 5 times until the resulting pH reached neutral, and dried at 50°C in air for 12 h. Finally, the porous TiO_2 nanowires were obtaind through calcination at 500°C in air atmosphere for 2 h.

2.2 Characterizations

X-ray diffraction (XRD) was carried out via Shimadzu XRD-6000 with high-intensity Cu Kα radiation. Field emission scanning electron microscopy (FESEM) were performed via Hitachi S-4800. Transmission electron microscopy (TEM) was carried out via high-resolution transmission electron microscopy (HRTEM, JEOL-2010 TEM with an acceleration voltage of 200 kV). Nitrogen adsorption-desorption measurements were recorded by Nova 2000E. The pore-size distribution was determined from the adsorption isotherm curves using the Barett-Joyner-Halenda (BJH) method.

2.3 Photocatalysis test

The process of photocatalytic experiments was performed as follows: 15 mg of porous TiO_2 nanowires or commercial TiO_2 powders were added into 50 mL MB or RhB aqueous solution whose concentration is 20 mg/L. Before irradiation, the above suspension first was ultrasonicated at 28°C for 30 min, followed by stirred in dark for ca. 30 min so as to get adsorption equilibrium of molecules. The mixture solution was exposed to ultraviolet (UV) light (Philips, 300 W, Shenzhen, China) with the intensity of 11280 μW/cm^2. The UV-light is 20 centimeters above the mixture solution. In the whole process of irradiation, the mixture was stirred without stop. After that, at a constant time interval, the mixture suspension (3.0 mL) was sampled and the catalyst particles were removed by centrifugation. The degradation rate of photocatalytic reaction was determined by UV-vis spectrophotometer (Tokyo, Japan, U-3010) through monitoring characteristic absorption of RhB (552 nm) and MB (665 nm).

3 Results and discussion

3.1 Structures and morphologies

Sodium titanate ($Na_2Ti_3O_7$) nanowire precursor was obtained by a hydrothermal method. The $Na_2Ti_3O_7$ nanowire precursor were washed with dilute HCl and then calcined to yield porous TiO_2 nanowires. Figure 1(a) presents the typical XRD pattern of the $Na_2Ti_3O_7$ nanowire precursor. It's clear that all peaks of the precursor belong to monoclinic phase $Na_2Ti_3O_7$ (JCPDS 72-0148) [19,20]. When the precursor was acid-washed and then treated by heating at 500°C in air for 2 h, the XRD diffraction peaks in Fig. 1(b) are totally different. All observed diffraction peaks conformed to the values of tetragonal phase TiO_2 (JCPDS 89-4921), which suggested the $Na_2Ti_3O_7$ nanowires precursor was transformed into tetragonal phase TiO_2 after acid-washed and being heated at 500°C in air. Scherer formula was adopted to estimate the average grain size of TiO_2 crystallites.

$$D = \frac{0.9\lambda}{\beta\cos\theta}, \tag{1}$$

where λ is the wavelength of the X-ray beam, θ is the diffraction angle and β is the full width at half maximum. The average TiO_2 crystallites size was ca. 10.7 nm.

Figure 2 displays the FESEM images of $Na_2Ti_3O_7$ nanowires and the corresponding TiO_2 product after acid-washed and heat-treatment. From Fig. 2(a), it can be seen that the precursors are a large amount of uniform nanowires. The length of $Na_2Ti_3O_7$ nanowires is from 2 to 8 μm. The diameter of the $Na_2Ti_3O_7$ nanowires is from 15 to 25 nm (Fig. 2(b)). Figures 2(c) and 2(d) display the FESEM images of the porous TiO_2 nanowires after acid-

1) 1 M = 1 mol/L

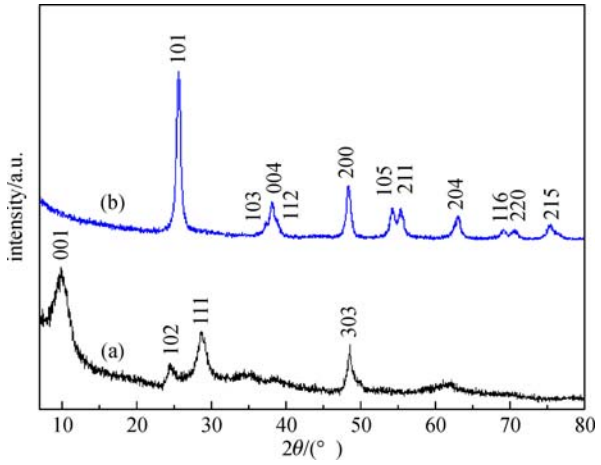

Fig. 1 XRD patterns of (a) $Na_2Ti_3O_7$ precursor and (b) TiO_2 product at 500°C for 2 h

washed and heat-treatment of the precursor. It can be clearly observed that after acid-washing and calcinations, no collapse occurred and the obtained product still maintained the wire-like shape similar to the precursor. Close observation further revealed that a vast of irregular nanopores exist randomly in the nanowires, which was resulted from the decomposition of nanowire precursor. The porous structure of TiO_2 materials has been further investigated by high-magnification and high-resolution TEM. The TEM image (Fig. 2(e)) reveals the nanowire-like architecture of the product. The high-magnification TEM image (Fig. 2(e) inset) indicates many nanopores distributed in the nanowires. From Fig. 2(f), it can be observed that the spacing of lattice fringe is approximate 0.24 nm, which is indexed with the (004) plane tetragonal phase TiO_2.

To study the texture of the porous TiO_2 nanowires, nitrogen adsorption/desorption measurements were conducted. Figure 3 displays the nitrogen adsorption/desorption isotherms and pore size distribution plot (inset) of the sample. The isotherm of sample shows a hysteresis loop at the p/p_0 ranges from 0.82 to 0.98 (Fig. 3), which is related to the filling up and emptying of mesopore by capillary condensation. The feature clearly suggests that the obtained sample possesses a large number of porosity. The BJH method originated from desorption branch of the nitrogen isotherm was applied to determine the pore size distribution of the porous TiO_2 nanowires. The result showed that the pore size of the as-prepared porous TiO_2 nanowires had an average diameter of 7.4 nm. The pore size distribution of the sample presents a broad peak with the range from 1.7 to 34.8 nm. Moreover, the FESEM images also verify the pores with different sizes in porous TiO_2 nanowires, which conform to the results of stochastic calculation. The surface area calculated of obtained sample is 86.4 $m^2 \cdot g^{-1}$. Because of the mesoporous structure and high surface area, the as-synthesized porous TiO_2 nanowires are more likely to provide a large amount of active sites on the surface of the material. Therefore, the as-synthesized porous TiO_2 nanowires are considered to have great potential application in photocatalytic degradation with superior performance.

3.2 Photocatalytic activities of the porous TiO_2 nanowires

To estimate the porous TiO_2 nanowires activity as the photocatalyst, the mixture was treated by UV light irradiation for a period of time. The intensity of absorption peak of the solution was measured to calculate photodagradation rate. When porous TiO_2 nanowires act as catalyst, during the process of irradiation, the absorbance spectra of RhB solution was shown in Fig. 4(a). It can be clearly observed that at 665 nm, the maximum absorbance decreases rapidly with increasing the irradiation time. After the mixture was irradiated by UV light for 7 min, the photodagradation rate reaches approximate 25.6%. After irradiation for 49 min, no obvious absorption peak was observed. The degradation ratio of RhB can be calculated using $1 - C_t/C_0$, where C_t is the concentration of dyes and C_0 is the initial concentration. The plots of irradiation time vs degradation ratio shows the degradation ratio of RhB can reaches up to 98.76%. Since no obvious absorption peak can be observed, the RhB in mixture can be considered to be almost totally decomposed. Figure 4(a) (inset) also exhibits photodagradation of RhB solution without any catalyst when the solution was exposed at different duration time under the same experiment condition. It's clearly found that after 49 min irradiation, there was almost no degradation in RhB solution, indicating that the as-synthesized porous TiO_2 nanowires are promising to act as excellent photocatalyst to remove RhB in water. Meanwhile, the plots of irradiation time vs degradation ratio were also achieved without catalyst, see Fig. 4(a) (inset). The result suggests that after the same duration time, no obvious degradation of RhB solution happened. Figure 4(b) shows characteristic absorption peak of MB solution with the catalyst. It clearly shows that the porous TiO_2 nanowires can serve as excellent catalyst for degradation of MB. Figure 4(b) (inset) demonstrates that the degradation ratio of MB solution reaches up to 97.98% after irradiation for 56 min. The photocatalytic performances of TiO_2 materials with different morphologies are listed in Table 1. The degradation ratio of the porous TiO_2 nanowires is higher than the previous reported values obtained under UV light irradiation with commercial TiO_2 powders (P25) [14], porous TiO_2 nanospheres [14], anatase nano-TiO_2 [21], and hierarchical TiO_2 nanoflowers [22]. Therefore, the as-prepared porous TiO_2 nanowires have great potential application in wastewater treatment. It is widely acknowledged that the catalytic process is primarily associated with the adsorption and desorption of molecules that usually occur on the surface of the catalyst. The possible reasons of the high performance TiO_2 nanowires may be ascribed to three

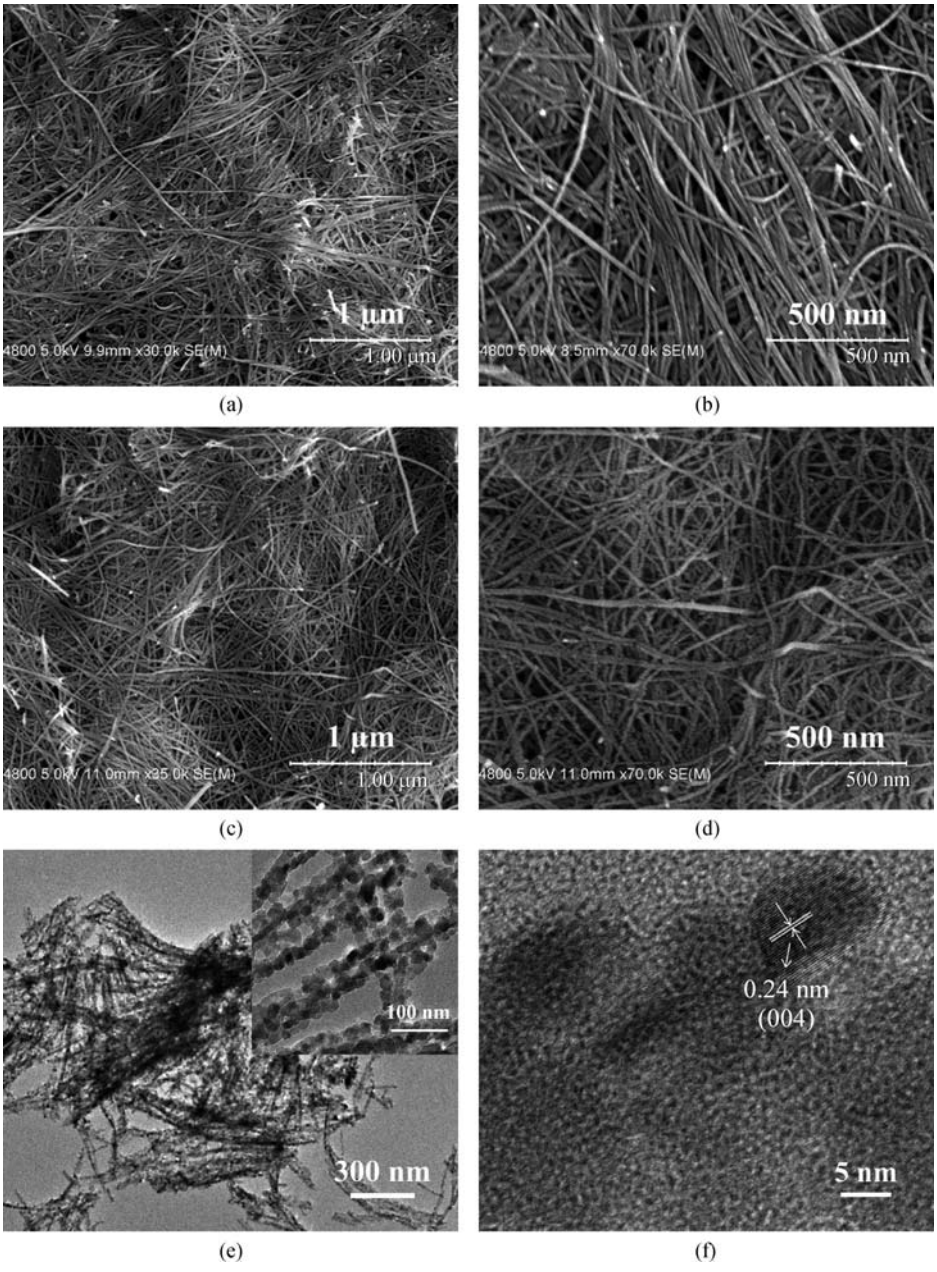

Fig. 2 Representative FESEM images of (a, b) the $Na_2Ti_3O_7$ nanowire precursor and (c, d) porous TiO_2 nanowires. (e) Typical TEM images and (f) HRTEM image of the porous TiO_2 nanowires. The inset is the corresponding TEM image at high magnification

aspects. First, the small size of nanocrystallites in the porous TiO_2 nanowires can effectively promote the transportation of carrier and greatly decrease the recombination rate between photoelectrons and holes, thus enhancing photocatalytic activities. Secondly, the porous structure of the TiO_2 nanowires facilitates the transportation of the pollutant molecules onto the surface of TiO_2 nanocrystallites and stores more molecules. Finally, the porous TiO_2 nanowires have the highest specific surface area than other catalysts, reaching up to 86.4 $m^2 \cdot g^{-1}$ (as shown in Table 1), which means it can produce more unsaturated surface coordination sites exposed to the solution, provide much more active reaction sites on the surface of material, and effectively promote the separation of electron–hole pairs, resulting in the high photocatalytic activities.

The reusability and stability of the sample are critical problems for developing practical application. The porous TiO_2 nanowires can be easily reused by centrifugation after each reaction. The reusability and stability of as-synthesized porous TiO_2 nanowires was tested through many times reusability of the catalyst. As can be seen in Fig. 5,

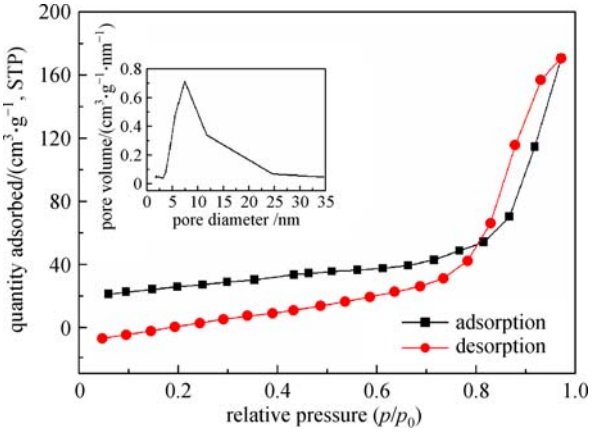

Fig. 3 N_2 adsorption-desorption isotherm and BJH pore size distribution plots (inset) of the porous TiO_2 nanowires. STP: standard temperature and pressure

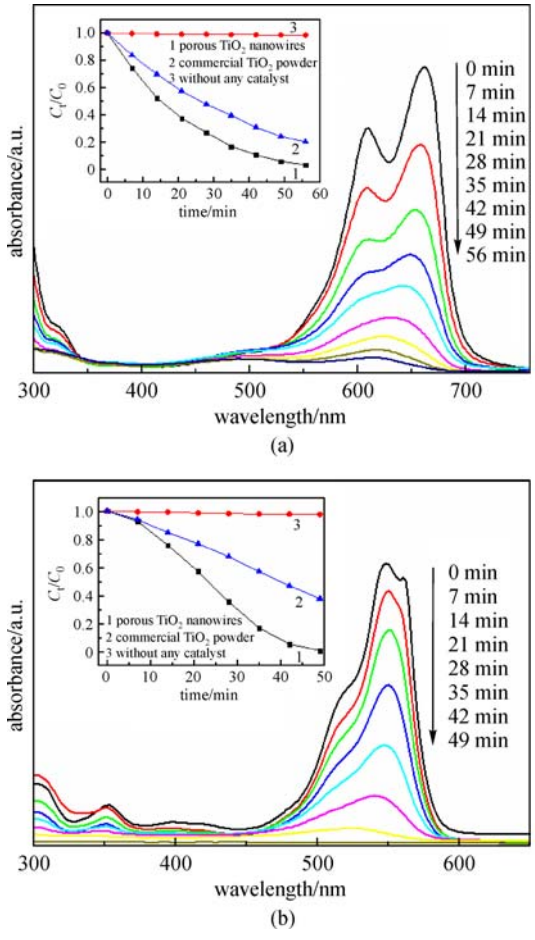

Fig. 4 Change of absorbance spectra of (a) RhB, (b) MB in solution with the concentration of 20 mg/L with porous TiO_2 nanowires under UV light irradiation. The insets are plots of photodegradation rate vs different irradiation time of RhB and MB under UV light irradiation with or without catalysts, where C_t is the concentration of dyes and C_0 is the initial concentration

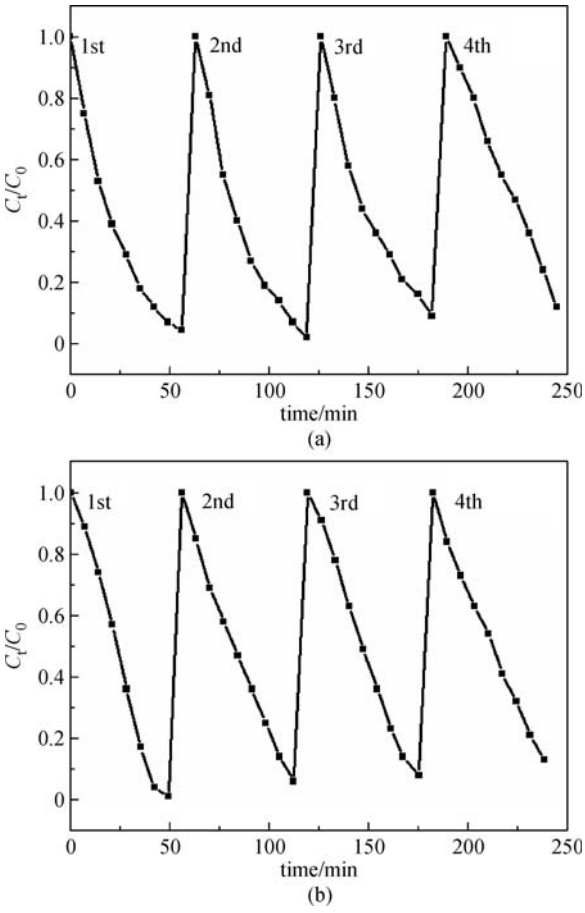

Fig. 5 Recycling results of the catalyst in the photodegradation of (a) MB, (b) RhB, in which C_t is the concentration of MB or RhB and C_0 is the initial concentration

after four cycling repeatability, the photocatalytic activity of catalyst do not show obvious decline and there are almost the same photodagradation rate in each cycle. Obviously, the porous TiO_2 nanowire prepared in this experiment is a promising photocatalyst due to its excellent photocatalytic activity and good recycle performance.

4 Conclusions

In conclusion, the synthesis of porous TiO_2 nanowires was successfully achieved through a hydrothermal method without any surfactant combined with acid-treatment and annealing process. Very high photodegradation efficiency (near 100%) for the degradation of MB and RhB was achieved by using porous TiO_2 nanowires as photocatalytic catalyst. The excellent photocatalytic activities can be ascribed to the small size of nanocrystallites, the porous structure and the larger specific surface area. Furthermore, the porous TiO_2 nanowires also show good stability in the process of degrading MB and RhB. Therefore, the porous

Table 1 Comparisons of the photocatalytic performances of TiO_2 materials with different morphologies

materials	specific surface area/($m^2 \cdot g^{-1}$)	pollutants	rate of degradation	Ref.
commercial TiO_2 powders	7.81	MB	48.2% (70 min)	[14]
		RhB	49.1% (70 min)	
corous TiO_2 nanospheres	26.1	MB	90.2% (70 min)	[14]
		RhB	98.1% (70 min)	
anatase nano-TiO_2	75.0	MB	90.3% (60 min)	[21]
		RhB	86.0% (60 min)	
hierarchical TiO_2 nanoflowers	35.8	RhB	97.8% (120 min)	[22]
porous TiO_2 nanowires	86.4	MB	97.98% (56 min)	this work
		RhB	98.76% (49 min)	

TiO_2 nanowire prepared in this work is a promising photocatalyst in the degradation of organic pollutants.

References

1. Khan S B, Hou M J, Shuang S, Zhang Z J. Morphological influence of TiO_2 nanostructures (nanozigzag, nanohelics and nanorod) on photocatalytic degradation of organic dyes. Applied Surface Science, 2017, 400: 184–193
2. Edy R, Zhao Y T, Huang G S, Shi J J, Zhang J, Solovev A A, Mei Y F. TiO_2 nanosheets synthesized by atomic layer deposition for photocatalysis. Progress in Natural Science-Materials International, 2016, 26(5): 493–497
3. Cheng G, Xu F F, Xiong J Y, Tian F, Ding J, Stadler F J, Chen R. Enhanced adsorption and photocatalysis capability of generally synthesized TiO_2-carbon materials hybrids. Advanced Powder Technology, 2016, 27(5): 1949–1962
4. Liu W G, Xu Y M, Zhou W, Zhang X F. A facile synthesis of hierarchically porous TiO_2 microspheres with carbonaceous species for visible-light photocatalysis. Journal of Materials Science & Technology, 2016, 33(1): 39–46
5. Zhang J Y, Li C X, Wang D Y, Zhang C, Liang L, Zhou X. The effect of different TiO_2 nanoparticles on the release and transformation of mercury in sediment. Journal of Soils and Sediments, 2017, 17(2): 536–542
6. Gaikwad M A, Mane A A, Desai S P, Moholkar A V. Template-free TiO_2 photoanodes for dye-sensitized solar cell via modified chemical route. Journal of Colloid and Interface Science, 2017, 488: 269–276
7. Qiu Y, Ouyang F. Fabrication of TiO_2 hierarchical architecture assembled by nanowires with anatase/TiO_2(B) phase-junctions for efficient photocatalytic hydrogen production. Applied Surface Science, 2017, 403: 691–698
8. Ma L Q, Xu W C, Zhu S L, Cui Z D, Yang X J, Inoue A. Anatase TiO_2 hierarchical nanospheres with enhanced photocatalytic activity for degrading methyl orange. Materials Chemistry and Physics, 2016, 170: 186–192
9. Goriparti S, Miele E, Prato M, Scarpellini A, Marras S, Monaco S, Toma A, Messina G C, Alabastri A, De Angelis F. Direct synthesis of carbon-doped TiO_2-bronze nanowires as anode materials for high performance lithium-ion batteries. ACS Applied Materials & Interfaces, 2015, 7(45): 25139–25146
10. Li X L, Bassi P S, Boix P P, Fang Y N, Wong L H. Revealing the role of TiO_2 surface treatment of hematite nanorods photoanodes for solar water splitting. ACS Applied Materials & Interfaces, 2015, 7 (31): 16960–16966
11. Praveen Kumar D, Lakshmana Reddy N, Karthikeyan M, Chinnaiah N, Bramhaiah V, Durga Kumari V, Shankar M V. Synergistic effect of nanocavities in anatase TiO_2 nanobelts for photocatalytic degradation of methyl orange dye in aqueous solution. Journal of Colloid and Interface Science, 2016, 477: 201–208
12. Hejazi S, Nguyen N T, Mazare A, Schmuki P. Aminated TiO_2 nanotubes as a photoelectrochemical water splitting photoanode. Catalysis Today, 2017, 281: 189–197
13. Yu W J, Liu Y M, Cheng N, Cai B, Kondamareddy K K, Kong S, Xu S, Liu W, Zhao X Z. Ultra-thin anatase TiO_2 nanosheets with admirable structural stability for advanced reversible lithium storage and cycling performance. Electrochimica Acta, 2016, 220: 398–404
14. Huang J R, Ren H B, Liu X S, Li X X, Shim J J. Facile synthesis of porous TiO_2 nanospheres and their photocatalytic properties. Superlattices and Microstructures, 2015, 81: 16–25
15. Ma J, Ren W H, Zhao J, Yang H L. Growth of TiO_2 nanoflowers photoanode for dye-sensitized solar cells. Journal of Alloys and Compounds, 2017, 692: 1004–1009
16. Lai L L, Wen W, Fu B, Qian X Y, Liu J B, Wu J M. Surface roughening and top opening of single crystalline TiO_2 nanowires for enhanced photocatalytic activity. Materials & Design, 2016, 108: 581–589
17. Yao Y C, Dai X R, Hu X Y, Huang S Z, Jin Z. Synthesis of Ag-decorated porous TiO_2 nanowires through a sunlight induced reduction method and its enhanced photocatalytic activity. Applied Surface Science, 2016, 387: 469–476
18. Bakar S A, Byzynski G, Ribeiro C. Synergistic effect on the photocatalytic activity of N-doped TiO_2 nanorods synthesised by novel route with exposed (110) facet. Journal of Alloys and Compounds, 2016, 666: 38–49
19. Myung S T, Takahashi N, Komaba S, Yoon C S, Sun Y K, Amine K, Yashiro H. Nanostructured TiO_2 and its application in lithium-ion storage. Advanced Functional Materials, 2011, 21(17): 3231–3241
20. Tsai C C, Teng H S. Structural features of nanotubes synthesized from NaOH treatment on TiO_2 with different post-treatments. Chemistry of Materials, 2006, 18(2): 367–373
21. Zhang J, Wu B, Huang L H, Liu P L, Wang X Y, Lu Z D, Xu G L,

Zhang E P, Wang H B, Kong Z, Xi J, Ji Z. Anatase nano-TiO_2 with exposed curved surface for high photocatalytic activity. Journal of Alloys and Compounds, 2016, 661: 441–447

22. Fan Z H, Meng F M, Zhang M, Wu Z Y, Sun Z Q, Li A X. Solvothermal synthesis of hierarchical TiO_2 nanostructures with tunable morphology and enhanced photocatalytic activity. Applied Surface Science, 2016, 360: 298–305

Yonglun Tang received his B.S. degree in Chemistry from the Chemistry Department of Anhui Normal University in 1983. He participated in the national seminar of Physical Chemistry in Nankai University in 1984. From 2002 to 2004, he attended in professional graduate course class of computer application technology in HeFei University of Technology. He is an associate professor of Inorganic Chemistry at Anhui Technical College of Industry and Economy. His present work mainly focuses on inorganic materials and photocatalyst.

Haibo Ren received his College degree in Chemistry from Hefei Normal University, Department of Chemical and Chemical Engineering, in 2010, meanwhile, B.S. degree in English from the English Department of Anhui University in 2011. He acquired his M.S. degree in Synthetic Inorganic Chemistry from the Chemistry Department of Anhui Normal University in 2015. He is currently working toward the Ph.D. degree at Yeungnam University in Korea. Now his work mainly focuses on the sensing materials and chemical sensors, photocatalyst, and secondary battery.

Jiarui Huang received his B.S. degree in Chemistry from the Chemistry Department of Anhui Normal University in 2000, his M.S. degree in Synthetic Organic Chemistry from the Chemistry Department of Nanjing University of Technology in 2003, and his Ph.D. degree in Inorganic Chemistry from the Chemistry Department of the University of Science and Technology of China in 2006. He is a professor of Inorganic Chemistry at Anhui Normal University. His present work mainly focuses on sensing materials, gas sensors, photocatalyst, and secondary battery.